Ionic loss from Venus through the solar wind interaction with the Venusian ionosphere

PRESENTED BY

Nora Ahmed El-Shafeay

Supervisors

Prof. Dr. Salah K. El-Labany
Professor of Theoretical Plasma Physics,
Physics Department, Faculty of Science,
Damietta University.

Prof. Waleed Moslem
Professor of Theoretical Plasma Physics,
Physics Department, Faculty of Science,
Port Said University.

Prof . Dr. Wael F. El-Taibany
Professor of Theoretical Plasma Physics,
Physics Department, Faculty of Science,
Damietta University.

OUTLINE

Introduction

Aim of the work

Research Plan

Physical Representation

Theoretical model

Wakefield potential

Results and discussion

Conclusion

Introduction

- **The solar wind** is a *supersonic plasma flow* that is mainly composed of protons ($\mathbf{H^+}$) and electron ($\mathbf{e^-}$) with a few percent of helium and some other heavier ionic species
- The high temperature of Sun's corona leads to the escaping of the solar plasma through the interplanetary space with dragging the solar magnetic field (interplanetary magnetic field).

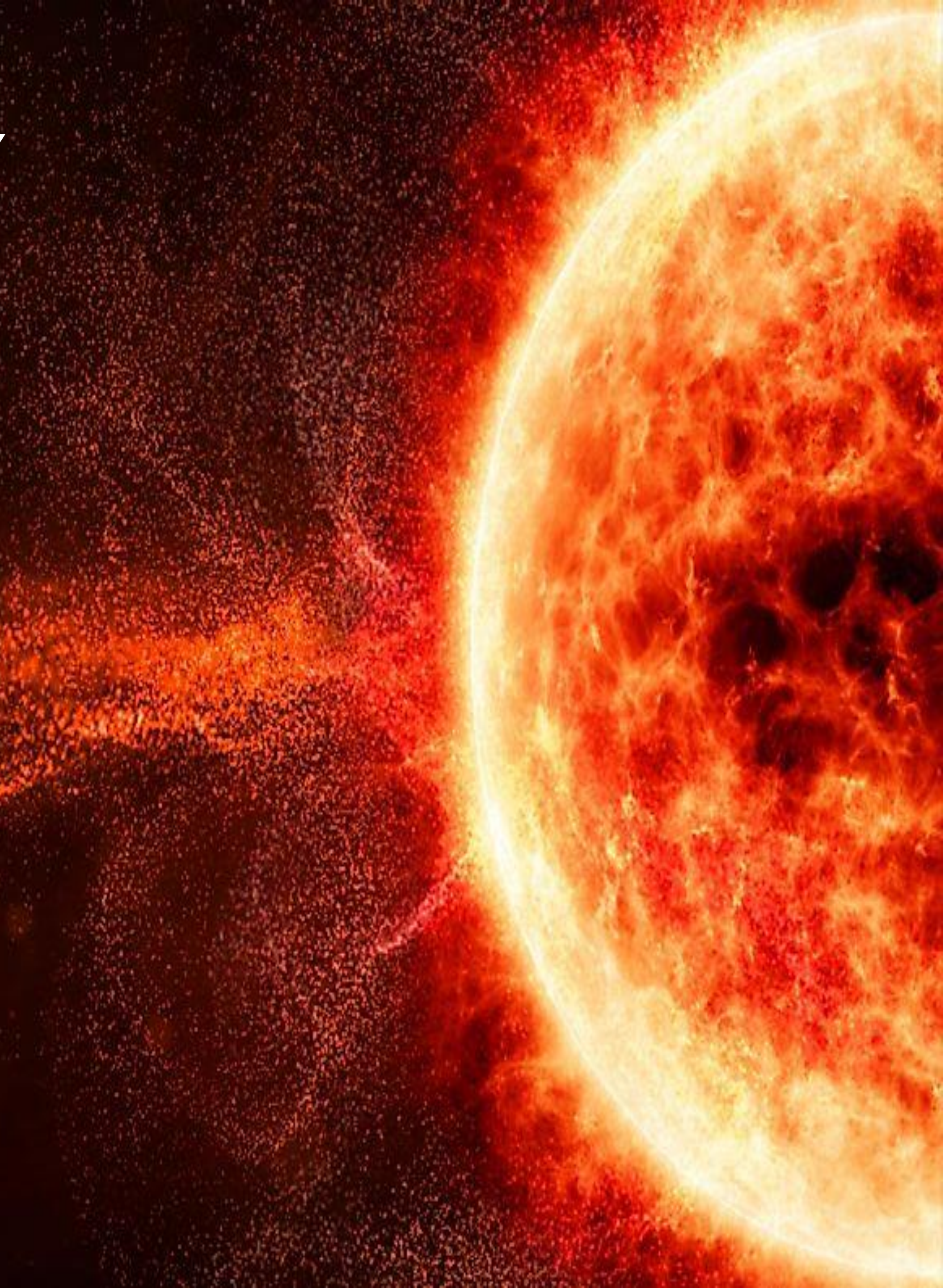

Planet Venus

- Venus is the second planet of our solar system, seen from the Sun.
- The planet Venus is one of the brightest objects on the night sky.
- Venus lacks an intrinsic magnetic field.
- Direct interaction between the solar wind and Venus.
- The solar wind controls the morphology and dynamics of the Venusian plasma environment.

Venus dayside synthesized false color image by UVI (2017 Jul 08).

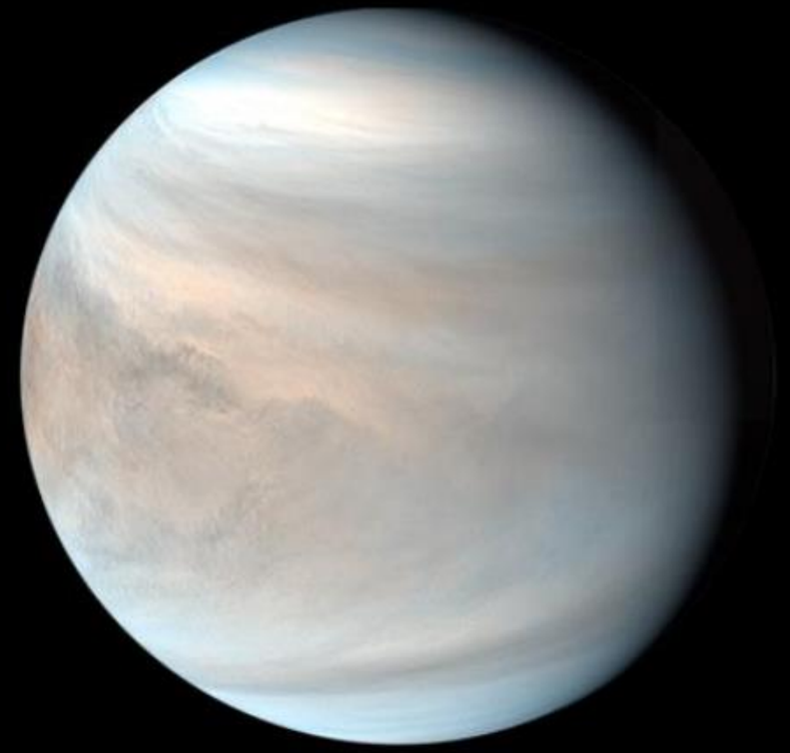

(C) Japan Aerospace Exploration Agency (JAXA (/PLANET-C Project Team

Planet Venus Cont.

- The atmosphere of Venus is crushingly thick, with a total mass 92 times that of Earth's atmosphere.
- It is mainly composed of carbon dioxide (96.5 %, CO_2).
- The CO_2 acts as a *greenhouse gas* that causes the lower atmosphere of Venus to have a temperature of above 460° C.
- In the upper atmosphere the CO_2 acts in an opposite manner. Here, it emits radiation, effectively cooling the upper atmosphere.

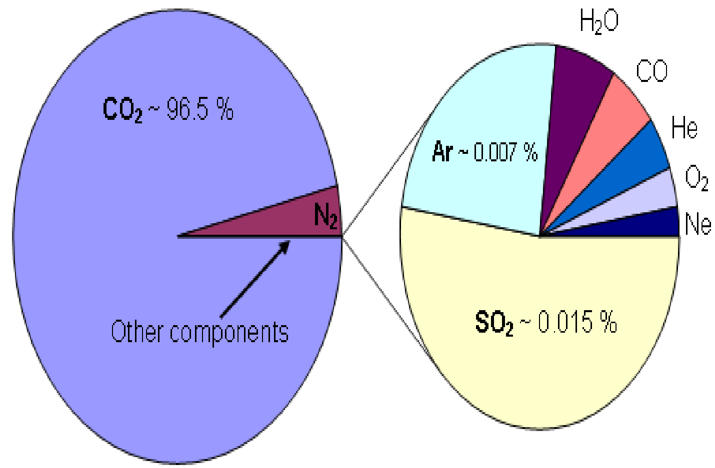

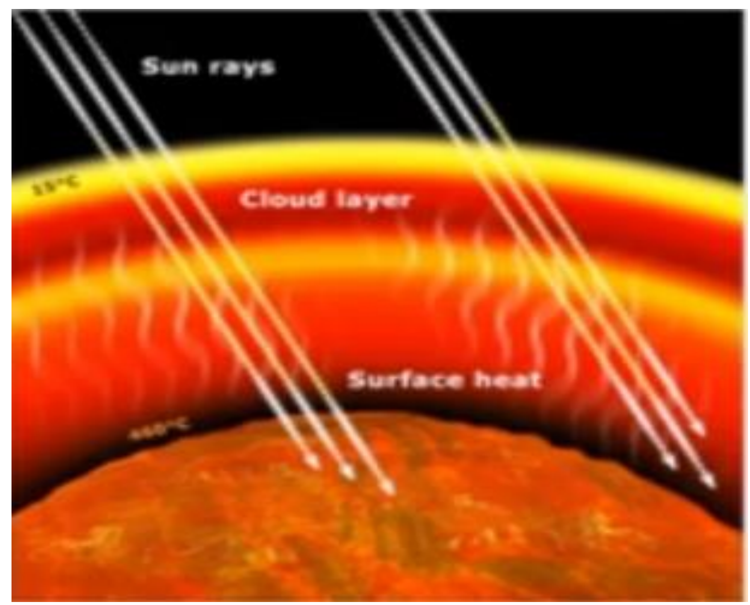

SW interaction with Venus

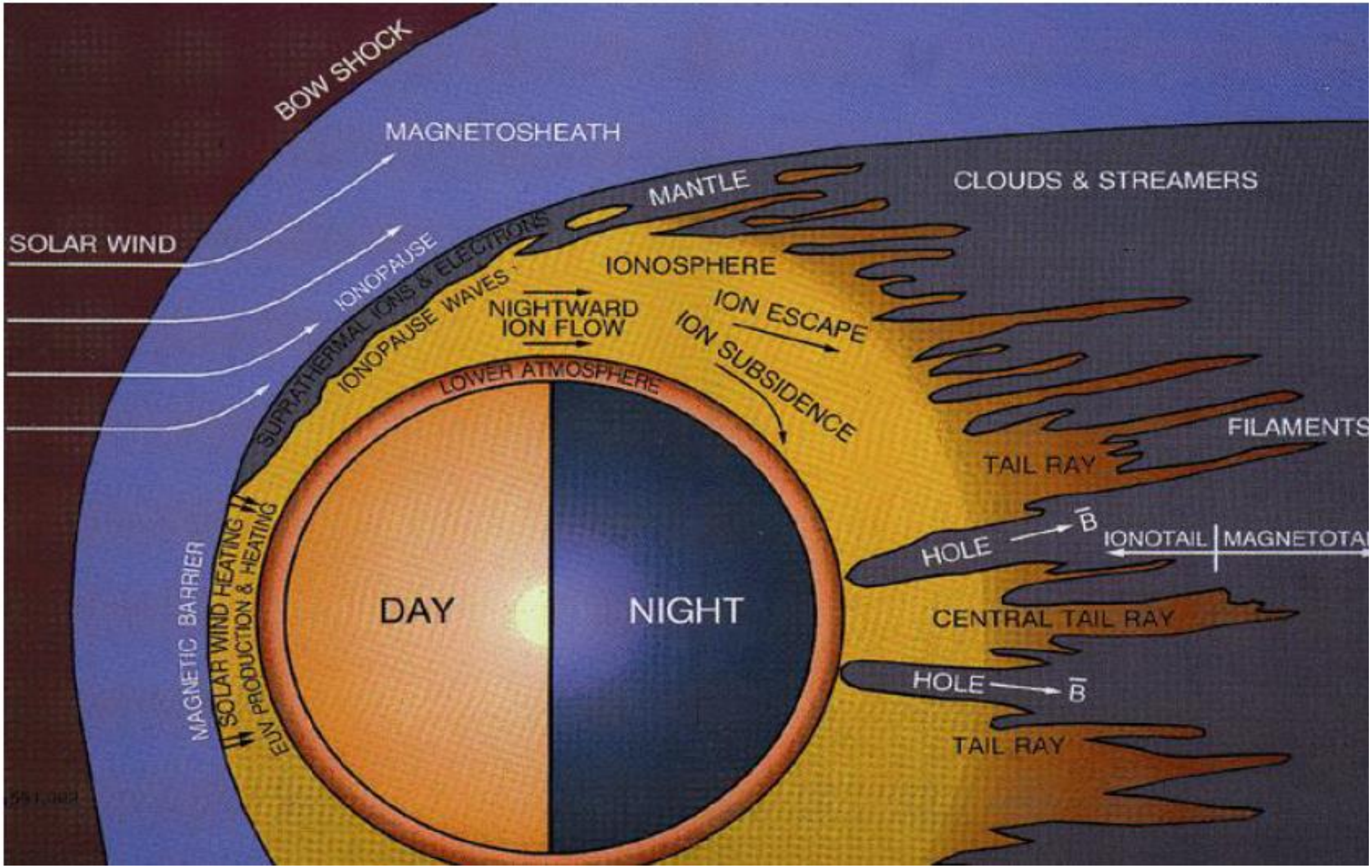

A sketch of the most important plasma boundaries and interaction regions in the environment of Venus

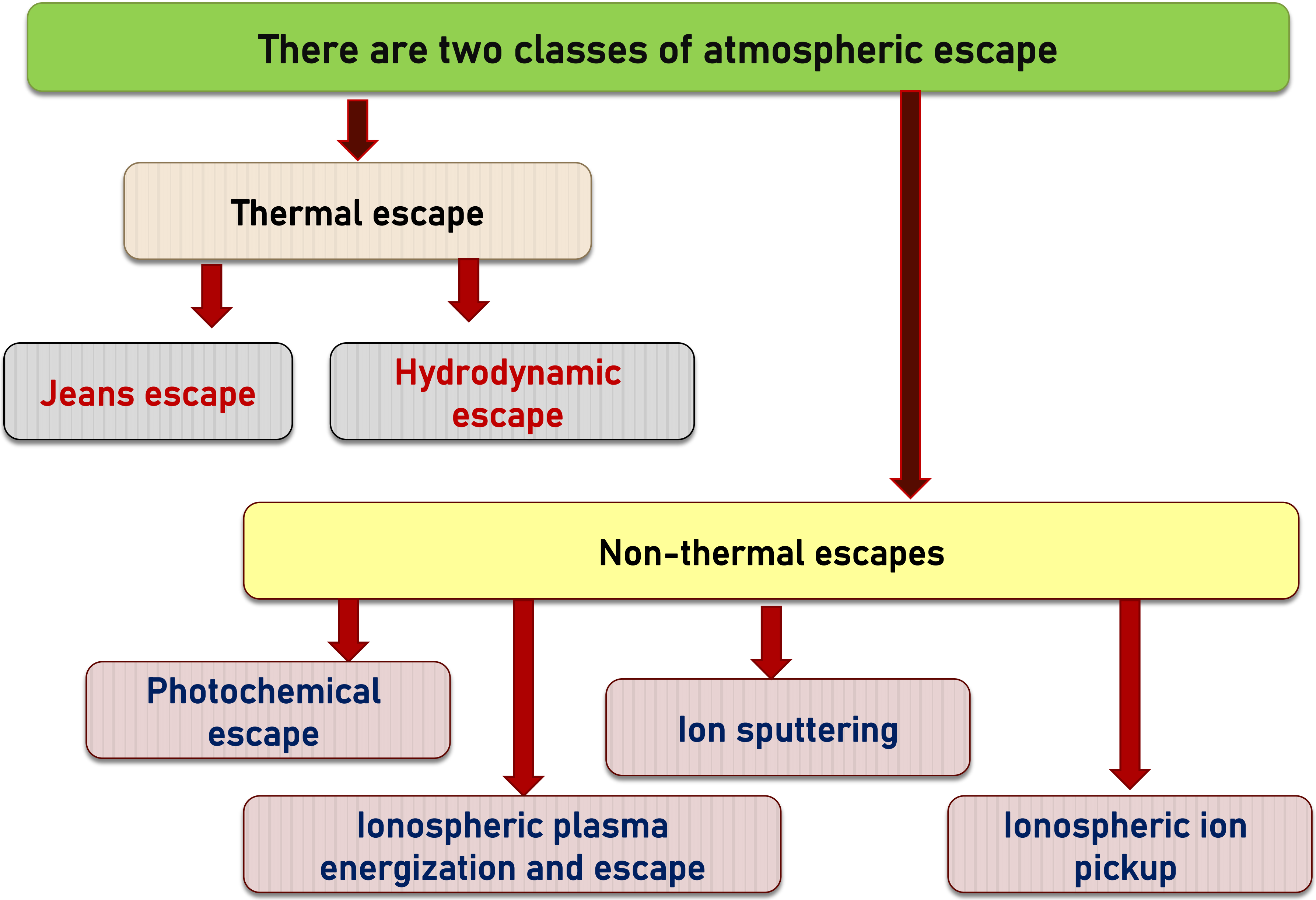
There are two classes of atmospheric escape
Thermal escape
Jeans escape
Hydrodynamic escape
Non-thermal escapes
Photochemical escape
Ion sputtering
Ionospheric plasma energization and escape
Ionospheric ion pickup

Aim of the work

Available online at www.sciencedirect.com
ScienceDirect
Advances in Space Research 65 (2020) 129–137
Advances in Space Research (a COSPAR publication)
www.elsevier.com/locate/asr

Ionospheric losses of Venus in the solar wind

S. Salem [a,b], W.M. Moslem [a,c,d,*], M. Lazar [d,e], R. Sabry [f,1], R.E. Tolba [c], R. Schlickeiser [d]

[a] Department of Physics, Faculty of Science, Port Said University, Port Said 42521, Egypt
[b] Basic and Applied Science Department, College of Engineering and Technology, Arab Academy for Science and Technology (AAST), Port Said, Egypt
[c] Centre for Theoretical Physics, The British University in Egypt (BUE), El-Shorouk City, Cairo, Egypt
[d] Institut für Theoretische Physik, Lehrstuhl IV: Weltraum- und Astrophysik, Ruhr-Universität Bochum, D-44780 Bochum, Germany
[e] Centre for Mathematical Plasma-Astrophysics, KU Leuven, Celestijnenlaan 200B, 3001 Leuven, Belgium
[f] Department of Physics, College of Science and Humanitarian in Al-Kharj, Prince Sattam bin Abdulaziz University, Al-Kharj 11942, Saudi Arabia

Received 15 July 2019; received in revised form 14 September 2019; accepted 18 September 2019
Available online 26 September 2019

Available online at www.sciencedirect.com
ScienceDirect
Advances in Space Research 68 (2021) 1525–1532
Advances in Space Research (a COSPAR publication)
www.elsevier.com/locate/asr

Ionic loss from Venus upper ionosphere via plasma wake

W.M. Moslem [a,b,*], I.A. Elsheikh [a,b], R.E. Tolba [b], A.A. El-Zant [b], M. El-Metwally [a]

[a] Department of Physics, Faculty of Science, Port Said University, Port Said 42521, Egypt
[b] Centre for Theoretical Physics, The British University in Egypt (BUE), El-Shorouk City 43, Cairo, Egypt

Received 1 July 2020; received in revised form 14 January 2021; accepted 23 March 2021
Available online 20 April 2021

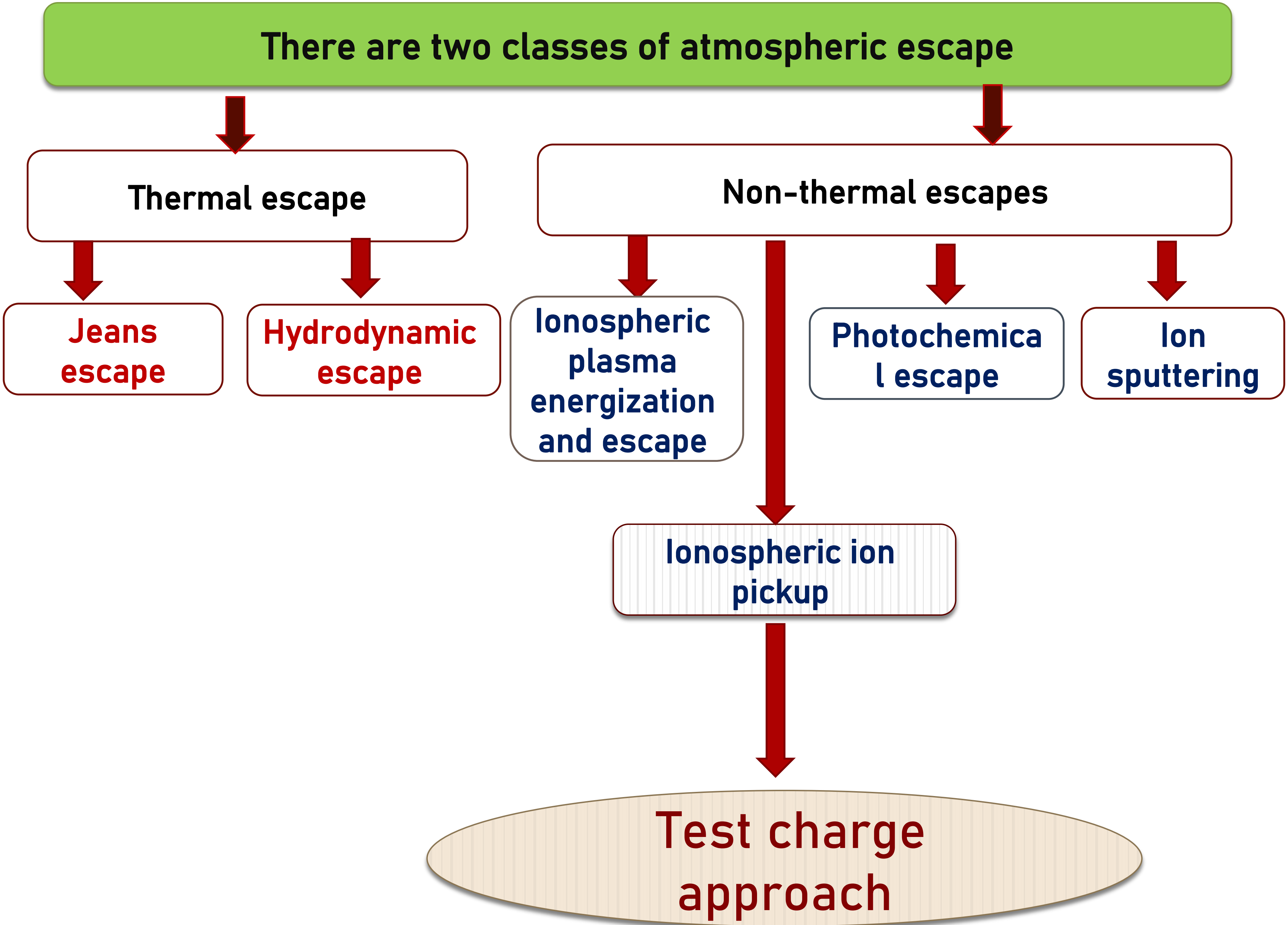
There are two classes of atmospheric escape
Thermal escape
Non-thermal escapes
Jeans escape
Hydrodynamic escape
Ionospheric plasma energization and escape
Photochemica l escape
Ion sputtering
Ionospheric ion pickup
Test charge approach

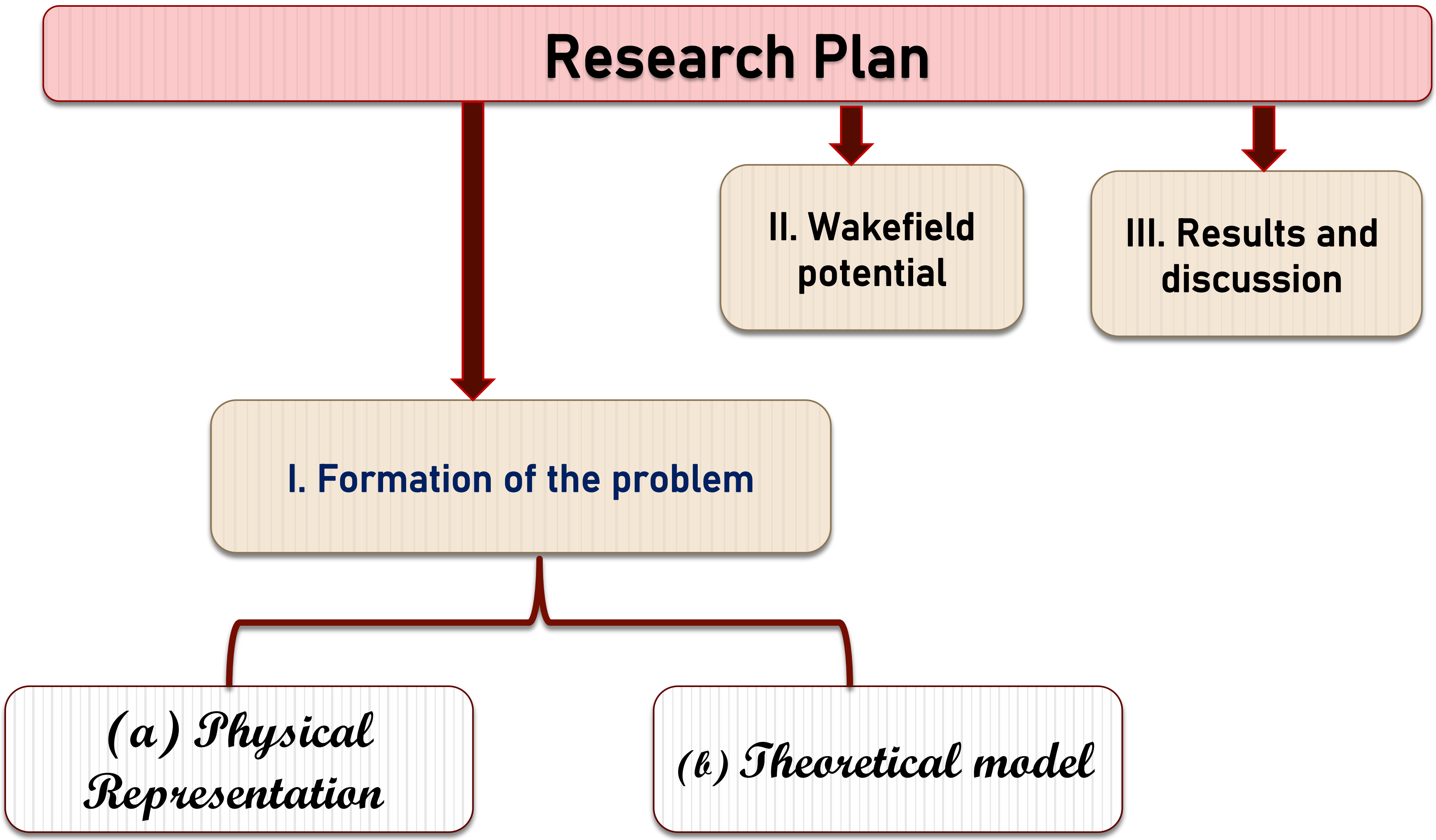
Research Plan
I. Formation of the problem
II. Wakefield potential
III. Results and discussion
(a) Physical Representation
(b) Theoretical model

(a) Physical Representation

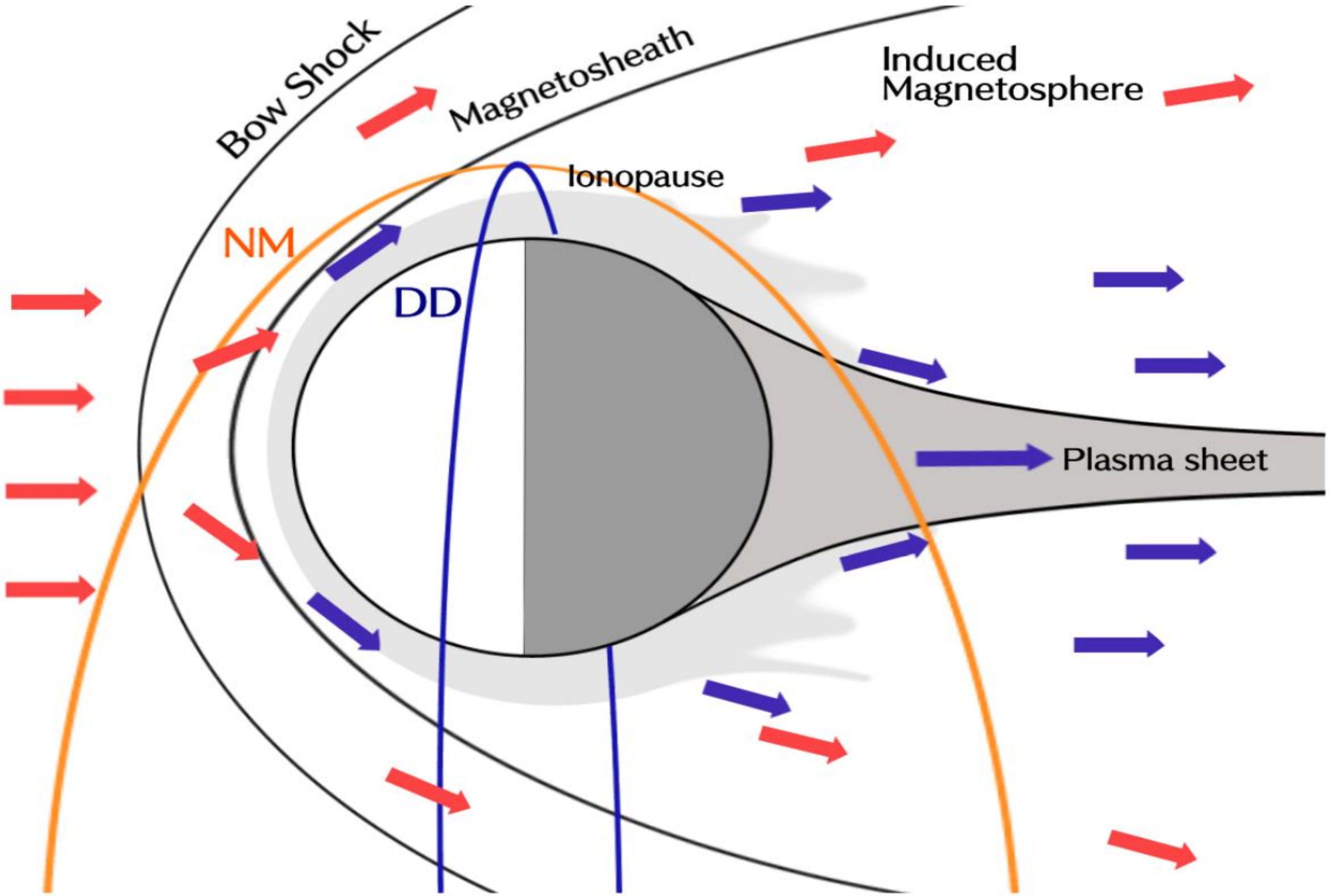

The **density** and **velocity** altitude profiles measured in the **Noon–Midnight** meridian at Venusian ionosphere by **Venus Express.**

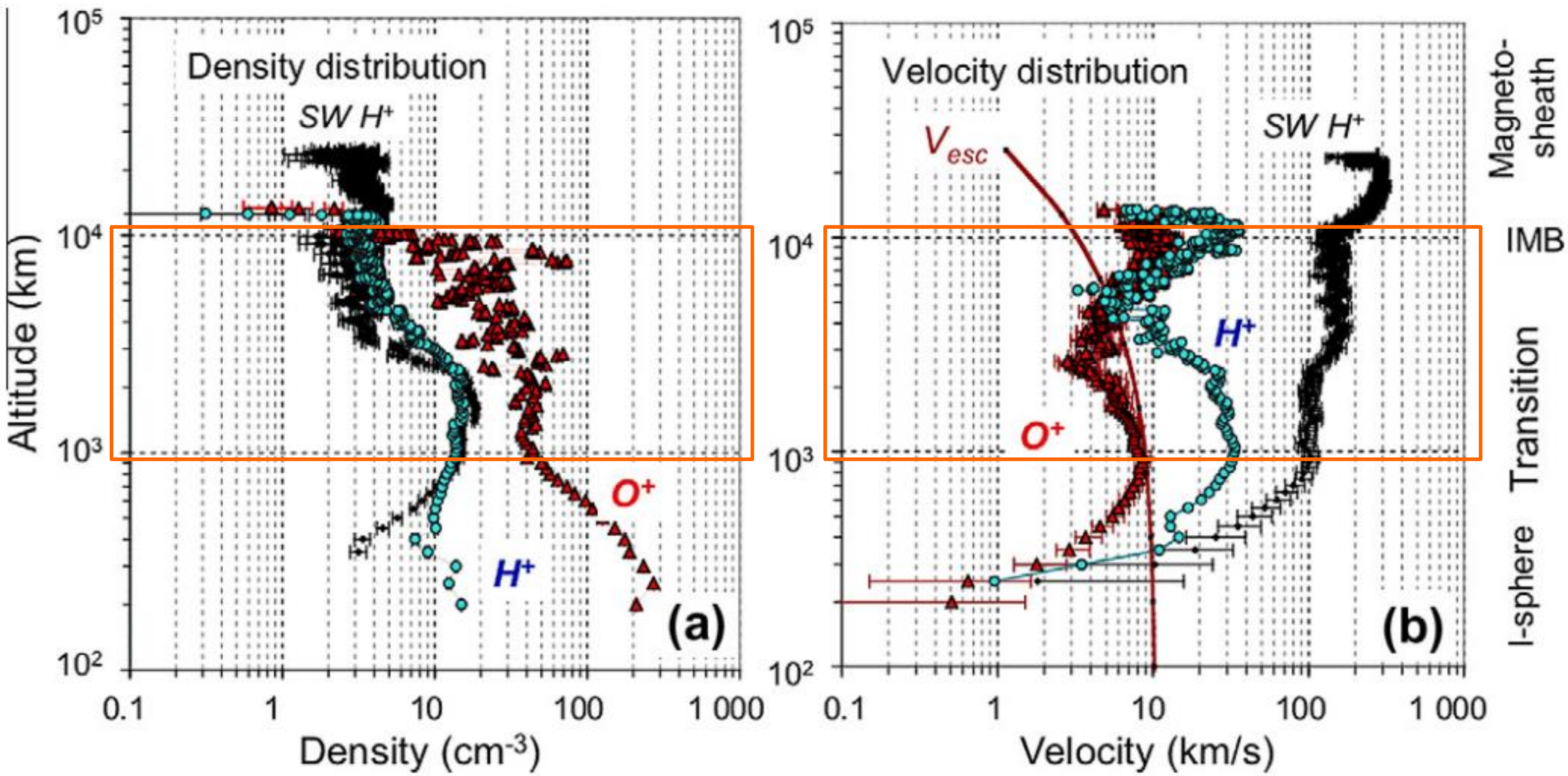

(b) Theoretical model

According to space observations, the fluids systems of equation are

$$\frac{\partial n_1}{\partial t} + \nabla.(n_1 \mathbf{u}_1) = 0, \qquad (1)$$

$$\left(\frac{\partial}{\partial t} + \mathbf{u}_1.\nabla\right)\mathbf{u}_1 + \underline{\frac{5}{3}\frac{n_1^{-1/3} k_B T_1}{m_1 n_{10}^{2/3}}}\nabla n_1 + \frac{e}{m_1}\nabla\phi = 0, \qquad (2)$$

Pressure gradient force

$$\frac{\partial n_2}{\partial t} + \nabla.(n_2 \mathbf{u}_2) = 0, \qquad (3)$$

$$\left(\frac{\partial}{\partial t} + \mathbf{u}_2.\nabla\right)\mathbf{u}_2 + \underline{\frac{5}{3}\frac{n_2^{-1/3} k_B T_2}{m_2 n_{20}^{2/3}}}\nabla n_2 + \frac{e}{m_2}\nabla\phi = 0, \qquad (4)$$

$$\frac{\partial n_{sp}}{\partial t} + \nabla.(n_{sp} \mathbf{u}_{sp}) = 0, \qquad (5)$$

$$\left(\frac{\partial}{\partial t} + \mathbf{u}_{sp}.\nabla\right)\mathbf{u}_{sp} + \underline{\frac{5}{3}\frac{n_{sp}^{-1/3} k_B T_{sp}}{m_{sp} n_{sp0}^{2/3}}}\nabla n_{sp} + \frac{e}{m_{sp}}\nabla\phi = 0, \qquad (6)$$

The isothermal electrons are

$$n_e = n_{e0}\exp(e\phi/k_B T_e), \tag{7}$$

$$n_{se} = n_{se0}\exp(e\phi/k_B T_{se}), \tag{8}$$

Finally, the system of equations (1)-(8) are closed by the Poisson equation which comprises both the plasma charge density, SW charge density, and the test charge density of a single test charge q_t, as

$$\nabla^2\phi = -4\pi\left[\rho_{plasma} + \rho_{test}\right]$$
$$= 4\pi e(n_e + n_{se} - n_1 - n_2 - n_{sp}) - 4\pi q_t \delta(r - v_t t) \tag{9}$$

At equilibrium, the neutrality condition is given by

$$n_{e0} + n_{se0} = n_{10} + n_{20} + n_{sp0}. \tag{10}$$

II. Wakefield potential

Applying space-time Fourier transformation to equations (1)–(8), we obtain the Fourier transformed number densities in ω–k space (ω is the wave frequency and k is the wave vector) as

$$n_{11} = \frac{e}{m_1}\frac{k^2 n_{10}}{R_1}, \qquad n_{21} = \frac{e}{m_2}\frac{k^2 n_{20}}{R_2},$$
$$n_{sp1} = \frac{e}{m_{sp}}\frac{k^2 n_{sp0}}{R_{sp}}, \qquad n_{se1} = \frac{e n_{se0}}{k_B T_{se}}\phi. \tag{11}$$
$$n_{e1} = \frac{e n_{e0}}{k_B T_e}\phi,$$

where

$$R_1 = \omega^2 - \frac{5}{3}k^2 v_1^2,$$
$$R_2 = \omega^2 - \frac{5}{3}k^2 v_2^2,$$
$$R_{sp} = (\omega - k.\mathbf{u}_{sp0})^2 - \frac{5}{3}k^2 v_{sp}^2,$$

Using the approximations $\omega < k.u_{sp0}$ into n_{sp0} and solving together with equation(9), we obtain the Fourier transformed electrostatic potential, as

$$\phi_1(k,\ \omega) = \frac{8\pi^2 q_t \delta(\omega - k.v_t)}{k^2 \varepsilon(k,\ \omega)} \tag{12}$$

$$\varepsilon(k,\ \omega) = \left[\frac{k^2\lambda_D^2 + 1}{k^2\lambda_D^2}\right]\left[1 - \frac{k^2\lambda_D^2}{k^2\lambda_D^2 + 1}\left(\frac{\omega_{p1}^2}{R_1} + \frac{\omega_{p2}^2}{R_2} + \frac{\omega_{p2}^2}{R_{sp}}\right)\right] \tag{13}$$

where

$$\lambda_D = [(\lambda_{D_e}^2 + \lambda_{D_{se}}^2)/\lambda_{D_e}^2\lambda_{D_{se}}^2]^{-1/2}, \qquad \lambda_{D_e} = (4\pi e^2 n_{e0}/K_B T_e)^{-1/2},$$

$$\lambda_{D_{se}} = (4\pi e^2 n_{se0}/K_B T_{se})^{-1/2}, \qquad \omega_{p1} = (4\pi e^2 n_{10}/m_1)^{1/2},$$

$$\omega_{p2} = (4\pi e^2 n_{20}/m_2)^{1/2}, \text{ and } \omega_{ps} = (4\pi e^2 n_{sp0}/m_{sp})^{1/2}$$

Taking the inverse Fourier transformation of equation(12), the electrostatic potential at an arbitrary position r becomes

$$\phi_1(\mathbf{r},\ t) = \frac{q_t}{2\pi^2}\int \frac{exp[ik.(r - \mathbf{v}_t t)]}{k^2\varepsilon(\mathbf{k},\ \omega)} d\mathbf{k}, \tag{14}$$

Inserting equation (13) into equation (14), and after straightforward algebraic manipulations, the Debye-Hückel and wakefied potentials can be simplified, respectively, as

$$\phi_D = \frac{q_t}{r} exp\left[\frac{-r}{\lambda_D}\right], \tag{15}$$

and

$$\begin{aligned}\phi_w(z,t) = \frac{2q_t}{z}&\left[1+\left(\frac{\omega_{p1}^2}{(v_t^2-\frac{5}{3}v_1^2)}+\frac{\omega_{p2}^2}{(v_t^2-\frac{5}{3}v_2^2)}+\frac{\omega_{ps}^2}{(u_{sp0}^2-\frac{5}{3}v_{sp}^2)}\right)\lambda_D^2\right]\\ &\times\left[1-\left(\frac{\omega_{p1}^2}{(v_t^2-\frac{5}{3}v_1^2)}+\frac{\omega_{p2}^2}{(v_t^2-\frac{5}{3}v_2^2)}+\frac{\omega_{ps}^2}{(u_{sp0}^2-\frac{5}{3}v_{sp}^2)}\right)\lambda_D^2\right]^{-1}\\ &\times cos\left[\left(\frac{\omega_{p1}^2}{(v_t^2-\frac{5}{3}v_1^2)}+\frac{\omega_{p2}^2}{(v_t^2-\frac{5}{3}v_2^2)}+\frac{\omega_{ps}^2}{(u_{sp0}^2-\frac{5}{3}v_{sp}^2)}\right)^{1/2} z\right]\end{aligned} \tag{16}$$

For effective **attraction,** it is necessary that the speed of moving charged particles **exceeds the acoustic speed.** In this case, the **collective effects** in multispecies plasma can optimally contribute to attraction between the ions. In general, in order for this to be operative, it is required that the wakefield potential (represented by Eq.(16)) is negative to obtain an **attractive wake potential**. This condition is satisfied when

$$\text{(i)} \quad \left[\left(\frac{\omega_{p1}^2}{(v_t^2 - \frac{5}{3}v_1^2)} + \frac{\omega_{p2}^2}{(v_t^2 - \frac{5}{3}v_2^2)} + \frac{\omega_{ps}^2}{(u_{sp0}^2 - \frac{5}{3}v_{sp}^2)}\right)\lambda_D^2\right] < 1,$$

and

$$\text{(ii)} \quad cos\left\{\left(\frac{\omega_{p1}^2}{(v_t^2 - \frac{5}{3}v_1^2)} + \frac{\omega_{p2}^2}{(v_t^2 - \frac{5}{3}v_2^2)} + \frac{\omega_{ps}^2}{(u_{sp0}^2 - \frac{5}{3}v_{sp}^2)}\right)^{1/2} z\right\} < 0.$$

For numerical analysis purposes, we make a suitable normalization of equations (15) and (16), where the potentials are by q_t/λ_D, the velocities normalized by $C_s = \omega_{p1}\,\lambda_D,$ and spatial distances by effective Debye length λ_D:

III. Results and discussion

Plasma parameters

Table 1: *Plasma parameters in the Venus' upper ionosphere for the Noon-Midnight meridian.*

Plasma parameters	At altitudes (1000 – 2000)	At altitudes (3000 – 10000)
Hydrogen density, n_{10} (cm^{-3})	10 – 18	14 – 3
Oxygen density, n_{20} (cm^{-3})	40 – 60	30 – 2
Solar wind proton density, n_{sp0} (cm^{-3})	16 – 20	7 – 2
Solar wind electron density, n_{se0} (cm^{-3})	16 – 20	7 – 2
Solar wind proton velocity, u_{sp0} (cm/s)	$(90-120)\times 10^5$	$(100-200)\times 10^5$

The temperatures are taken as $T_e = 10\times 10^4 K$**,** $T_1 = T_2 = 2\times 10^4 K$**,** $T_{sp} = (10-25)\times 10^4 K$, and $T_{se} = (10-35)\times 10^4 K$ **(Lundin et al. 2011, Knudsen et al. 2016).**

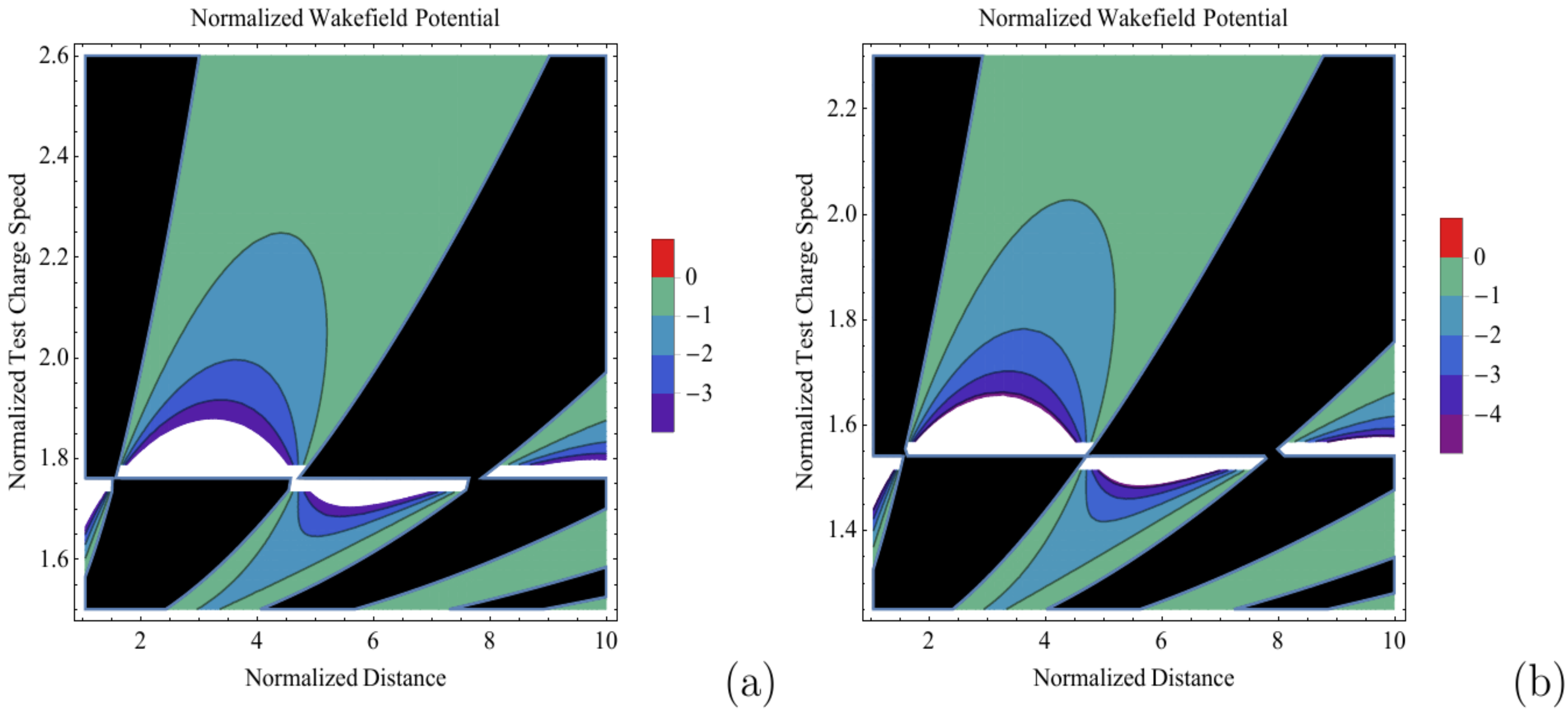

Figure 1: The countourplot of the normalized wakefield potential in terms of the normalized axial distance and normalized test charge speed at altitudes (a) 1000 km and (b) 10000 km (***Noon–Midnight*** meridian).

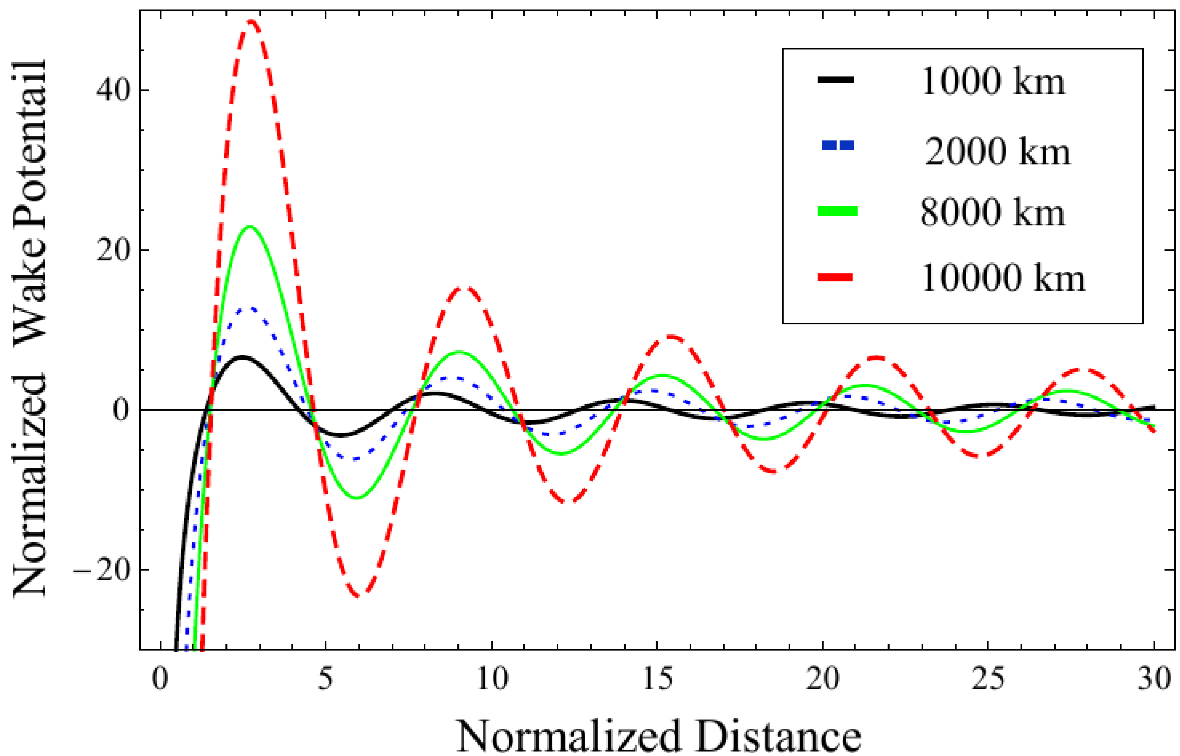

Figure 2: The normalized wakefield potential is depicted against the normalized axial distance for different altitudes. Here the normalized test charge velocity is $\bar{v}_t = 1.6$.

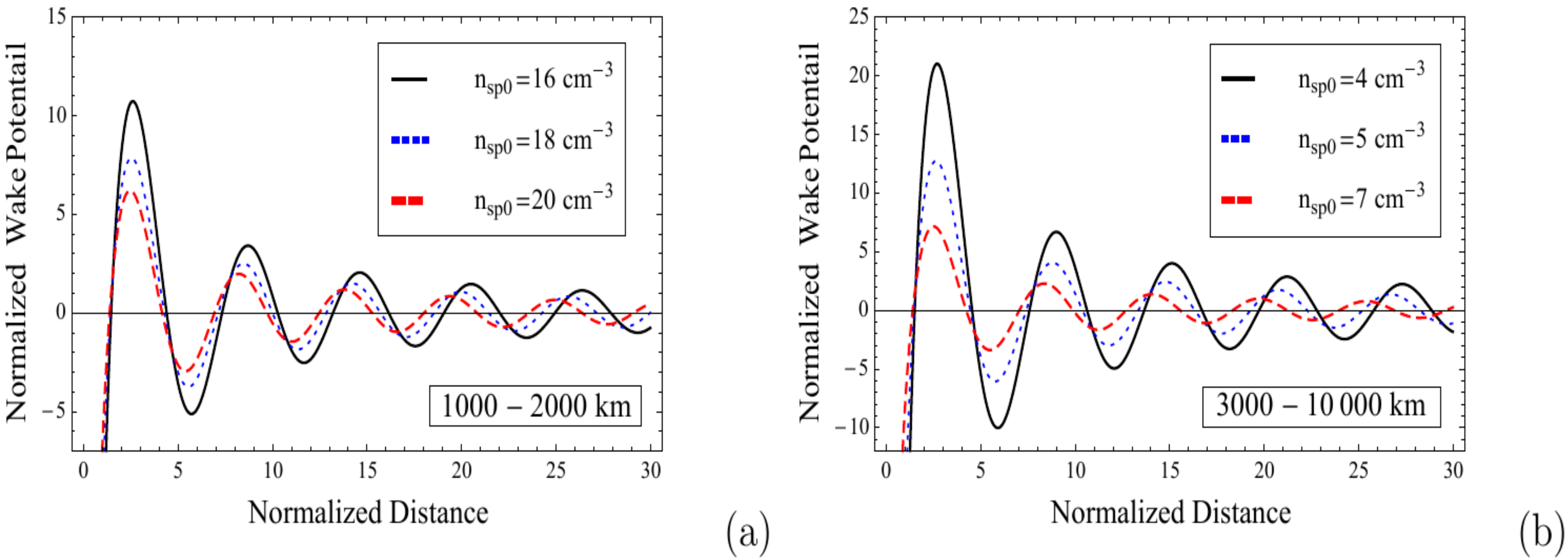

Figure 3: The normalized wakefield potential is depicted against the normalized axial distance for different values of n_{sp0} at altitudes (a) 1000-2000 km (transition region) with $\bar{v}_t = 1.7$ and (b) 3000-10000 km with $\bar{v}_t = 1.5$.

The density and velocity altitude profiles measured in the Noon–Midnight meridian at Venusian ionosphere by Venus Express.

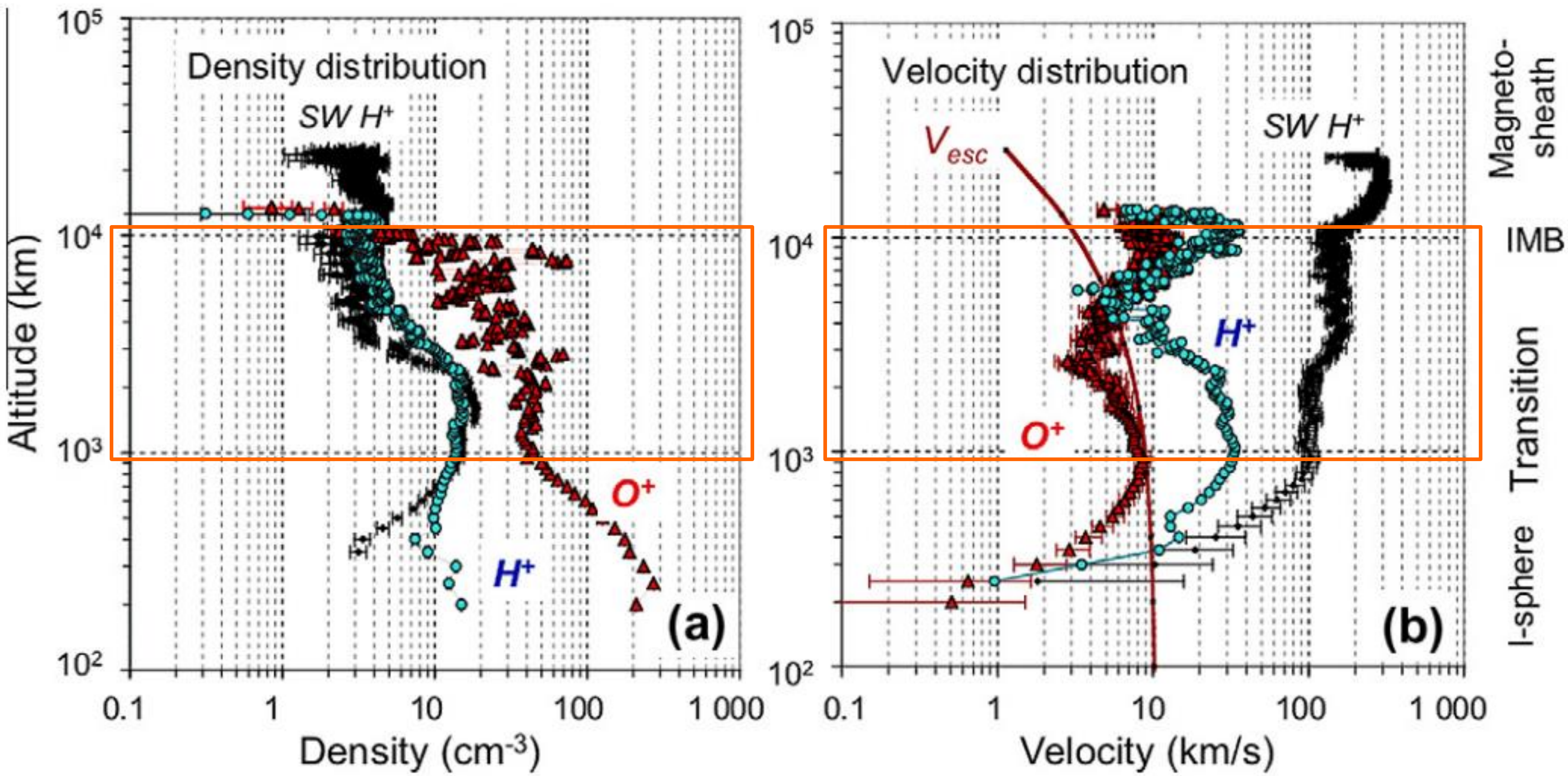

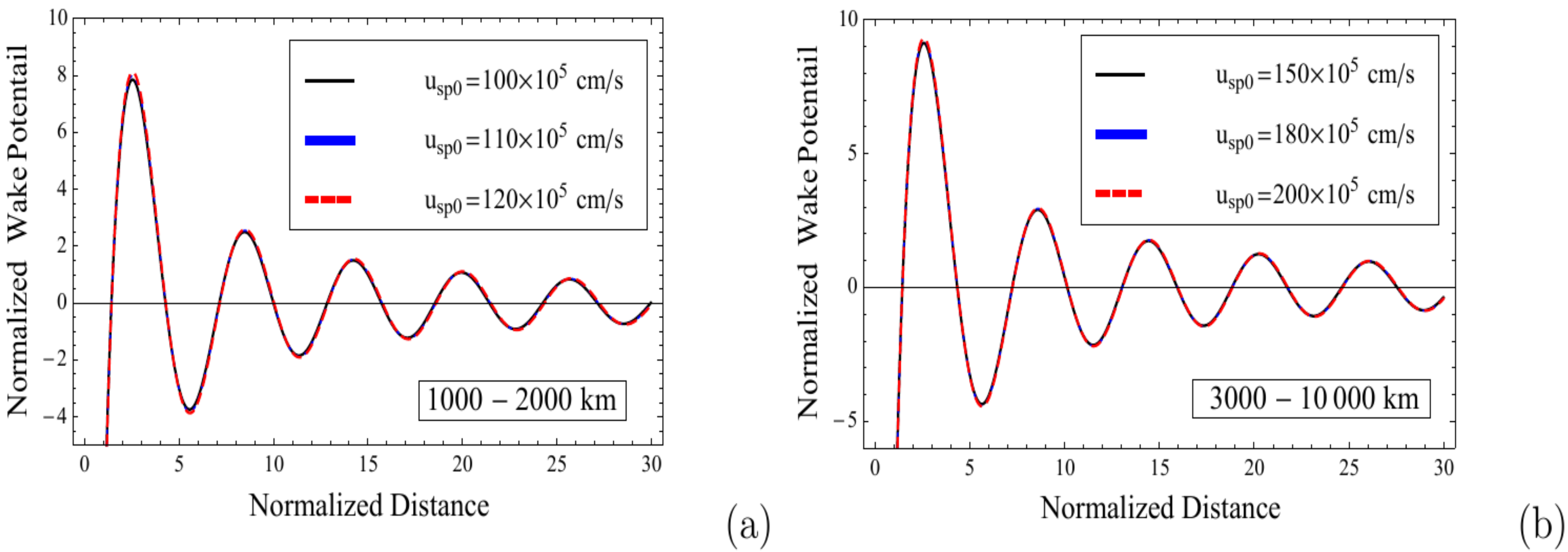

Figure 4: The normalized wakefield potential is depicted against the normalized axial distance for different values of u_{sp0} at altitudes (a) 1000-2000 km (transition region) with $\bar{v}_t = 1.7$ $(\boldsymbol{v_t}\boldsymbol{=}\ (\mathbf{20-22}) \times \mathbf{10^5}\boldsymbol{cm/s})$ and (b) 3000-10000 km with $\bar{v}_t = 1.5$ $(\boldsymbol{v_t}\boldsymbol{=}\ (\mathbf{15-30}) \times \mathbf{10^5}\boldsymbol{cm/s})$.

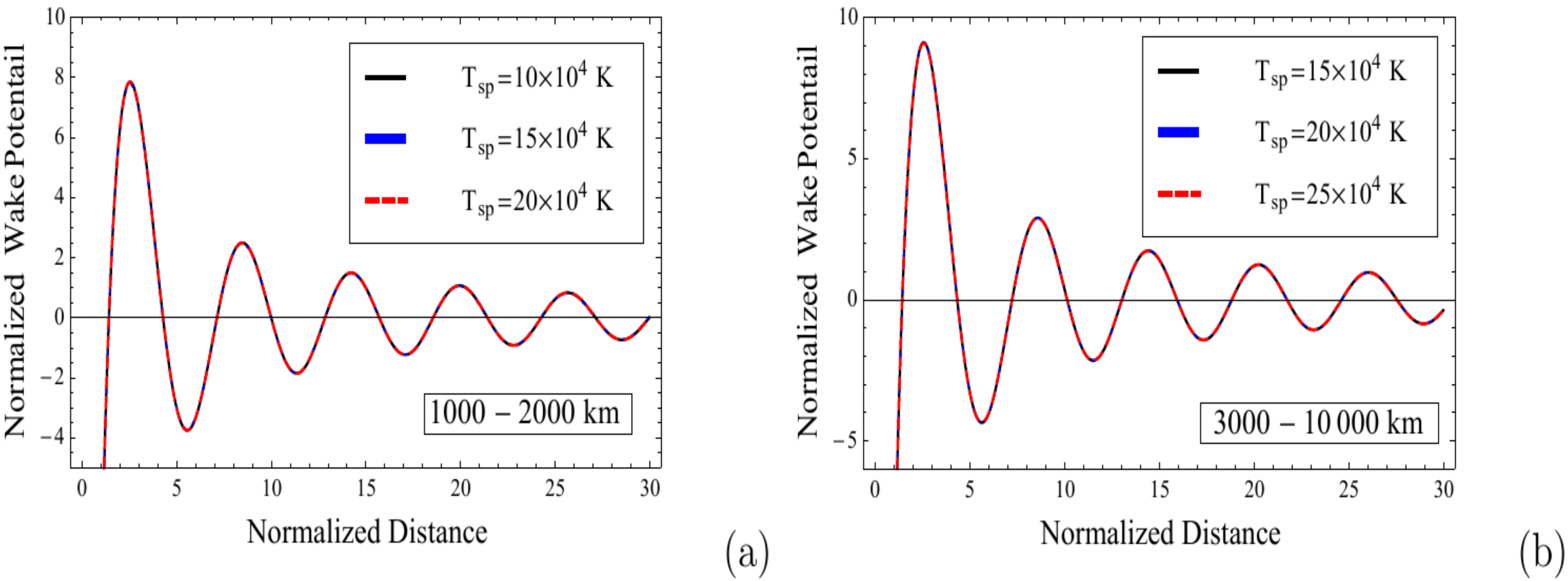

Figure 5: The normalized wakefield potential is depicted against the normalized axial distance for different values of T_{sp} at altitudes (a) 1000-2000 km (transition region) with $\bar{v}_t = 1.7$ and (b) 3000-10000 km with $\bar{v}_t = 1.5$.

Conclusion

- We have presented an additional mechanism, involving an attractive wakefield potential between like charges, to explain the ionic loss in Venus.
- Regions of both attractive and repulsive potentials were delineated at different altitudes.
- Our results show that the enhancement of Wakefield amplitudes with increasing the altitude. Which means we would observe significant ionic loss rates at higher altitudes.
- The SW protons density (n_{sp0}) dimensions the amplitude of the wakefield potential at transition region (1000-2000 km). In contrast, the n_{sp0} enhances the amplitude of the wakefield potential for higher altitudes (> 2000 km).
- The streaming SW velocity and the temperature still have no effect on the wakefield potential (plasma escaping).
- Our results are in agreement with trends inferred from the VEX observations in *Lundin et al., 2011*.

Thank you